Quark-cluster-model predictions for the nuclear Drell-Yan process

A. Harindranath and J. P. Vary
Physics Department, Iowa State University, Ames, Iowa 50011
(Received 8 April 1986)

We evaluate the quark-cluster-model predictions for lepton pair production in proton-nucleus, pion-nucleus, and nucleus-nucleus interactions. We examine the issue of a possible ambiguity between the K factor and the probability of six-quark clusters in nuclei. We present predictions for cross sections and cross-section ratios which show substantial sensitivity to different features of the model. The model compares well with the existing data.

INTRODUCTION

Several authors[1-5] have proposed that the study of lepton pair production in hadron-nucleus reactions, the Drell-Yan (DY) process,[6] can generate constraints on models that explain deep-inelastic lepton-nucleus scattering (DIS) experiments (Refs. 7–13). Under optimal circumstances, information from the DY process can also be utilized to discriminate between these models. In this work we primarily evaluate nuclear effects on the DY process within the quark-cluster model (QCM) (Refs. 14–16). Our major goal here is to elucidate those kinematic regions which show maximal sensitivity to different features of the QCM.

The plan of this paper is as follows. In Sec. I we summarize our notation and the various forms for the double-differential cross section. In Sec. II we review the QCM and its ingredients. Results for the nucleon-nucleus DY process are given in Sec. III. Section IV surveys the pion-nucleus DY process and the nucleus-nucleus DY process is discussed in Sec. V. Finally, we present our conclusions.

I. DY CROSS SECTION

In the hadron-hadron center-of-momentum frame we denote the total energy by $\sqrt{s}$. For hadrons A and B the four-momenta are $P_A=(\sqrt{s}/2,0,0,\sqrt{s}/2)$ and $P_B=(\sqrt{s}/2,0,0,-\sqrt{s}/2)$. Let x_1 (x_2) denote the fraction of longitudinal momentum carried by quark 1 (2) in hadron A (B). Then the longitudinal momentum of the lepton pair with invariant mass M is given by

$$P_L=p_1+p_2=(x_1-x_2)\frac{\sqrt{s}}{2} .$$

The kinematical variable $\tau\equiv x_1x_2$ becomes M^2/s since we are consistently neglecting the transverse momentum of the lepton pair. Then

$$P_L=\left[x_1-\frac{M^2}{sx_1}\right]\frac{\sqrt{s}}{2}$$

yielding

$$P_L^{\max}=\left[1-\frac{M^2}{s}\right]\frac{\sqrt{s}}{2} .$$

We also employ

$$x_F=\frac{P_L}{P_L^{\max}}=\frac{x_1-x_2}{(1-\tau)} .$$

Experiments measure laboratory quantities sufficient to determine M, P_L, and the lepton-pair transverse momentum P_T. We consider only P_T-integrated cross sections.

According to the naive DY model[6] the differential cross section for the process $AB\Rightarrow\mu^+\mu^-X$ is given by

$$\frac{d\sigma}{dM^2}=\frac{4\pi\alpha^2}{9M^2}\sum e_a{}^2\int dx_1dx_2F_a(x_1,x_2)\delta(M^2-x_1x_2s) ,$$

where

$$F_a(x_1,x_2)=q_a^A(x_1)\bar{q}_a^B(x_2)+\bar{q}_a^A(x_1)q_a^B(x_2) .$$

Here summation is over the flavor index a. Further, q_a^A is the quark distribution of flavor a in hadron A and $\bar{q}_a^B$ is the antiquark distribution of flavor a in hadron B. Thus

$$\frac{d^2\sigma}{dx_1dx_2}=\frac{4\pi\alpha^2}{9sx_1x_2}\sum e_a{}^2F_a(x_1,x_2) .$$

Data are sometimes presented after transforming to the variables x_F and M, yielding

$$\frac{d^2\sigma}{dM^2dx_F}=\frac{4\pi\alpha^2}{9M^4}(1-\tau)\sum e_a{}^2\frac{x_1x_2}{x_1+x_2}F_a(x_1,x_2) .$$

The DY process corresponds to the smooth part of the dilepton pair cross section in the $M\geq 4$ GeV region. It does not account for the known massive resonances present in this region. Therefore comparisons with data in the $M\sim 4$ GeV region could be obscured by contributions from the J/ψ resonance.

II. SPECIFICATION OF THE MODEL

The QCM (Refs. 14–16) assumes the scattered quark originates from a color-singlet cluster composed of 3, 6, 9, etc., valence quarks. Clusters are defined by the "overlap" of three-quark ($3q$) subsystems, each of which is assigned a critical radius R_c. Overlap is assumed to occur when two subsystems are separated by a distance $\leq 2R_c$. The position of each $3q$ subsystem is determined by the nuclear wave functions with pointlike nucleons. Then if $R_c=0$, no quark clusters larger than nucleons are formed,

and the standard model of the nucleus survives. If R_c is large, say $\sim 1.0-1.2$ fm, then percolation occurs, and the nucleus has a high probability of being found in a $3A$ quark-cluster configuration. In fits to DIS, the value $R_c = 0.50 \pm 0.05$ fm provides a reasonable description of the data on ^{3}He and a qualitative description of the European Muon Collaboration (EMC) (Ref. 7) and SLAC (Ref. 8) data.

For the QCM we employ the quark distributions of Carlson and Havens[15] which differ in minor ways from those first proposed.[14] Recently, results for quark-cluster probabilities in a wide range of nuclei have been obtained[17] for $R_c = 0.50$ fm. For light nuclei the probabilities are calculated using realistic nuclear wave functions. Through a study of the density dependence of these results one obtains $3q$, $6q$, $9q$, and $12q$ cluster probabilities in heavy nuclei. For the purpose of the present work we consider only the role of $3q$ and $6q$ clusters. Denoting the $3q$ cluster probability as p_3 we take the $6q$ cluster probability p_6 as $p_6 = 1 - p_3$, where p_3 is taken from Ref. 17. As an example, for Fe we get $p_6 = 0.186$ to be compared with 0.3 used by Carlson and Havens. We summarize in Table I the values for $p_6 = 1 - p_3$ for those nuclei occurring as targets or projectiles in the present work.

We have neglected the Fermi-motion effects, which are known to be important in the QCM around $x = 1$.

III. NUCLEON-NUCLEUS DY PROCESS

A. Model results and p_6 dependence

The expression for the DY cross section depends on a product of quark momentum distribution functions as opposed to the linear dependence appearing in DIS cross section. By focusing on selected values of projectile x_1, the DY process can provide new information regarding target distribution functions. Projectile valence terms are dominant for $x_1 > 0.3$ and projectile sea distributions are dominant for small values of x_1. Thus at large x_1 the DY process can be a new source of information about the antiquark distributions of the target nucleus.

Because of the assumptions of QCM, the valence quarks carry a smaller fraction of the total momentum in a $6q$ system than in a $3q$ system. If we assume that the gluons carry the same momentum fractions in all clusters then a certain enhancement of the sea's momentum fraction is required to conserve total momentum.[15] We adopt this assumption for the present work in concert with the assumptions of Carlson and Havens.[15]

In Fig. 1 we present the ratio of DY cross sections for Fe and D as a function of x_2 for two characteristic values of x_1. Small values of x_1 yield a ratio of cross section similar to the ratio of valence-quark contributions in the DIS cross section.[15,16] Large values of x_1 yield a ratio of the sea-quark contributions which display the enhancement arising from the assumed gluon behavior. Clearly, if data can be obtained at different values of x_1 it would be possible to separately test the valence and sea distributions within the QCM.

The importance of having independent tests of the valence- and sea-quark contributions is highlighted by the different descriptions of the low-x region that have appeared. To *fit* the EMC (Ref. 7) data at low x the authors of Ref. 15 found it necessary to emphasize the role of $6q$ clusters by having the $6q$ admixture as large as 30% in Fe and zero admixture in D. This had the net effect of giving a much more prominant role to the enhanced $6q$ sea. We have consistently employed the quark cluster probabilities determined by other data sets (Refs. 14 and 17) which imply $p_6(\text{Fe}) \simeq 0.18$ and $p_6(\text{D}) \simeq 0.04$ and have therefore "underpredicted" the low-x Fe/D ratio. However, new Bologna-CERN-Dubna-Munich-Saclay[9] (BCDMS) data on the low-x N/D ratio is very close to unity. This again raises questions on the normalization of the EMC (Ref. 7) data.

In Figs. 2(a)–2(d) the ratio of cross sections for Al and Au to D are presented as functions of the variables M and x_F. In Figs. 2(a) and 2(b) large enhancements appear in

TABLE I. Six-quark cluster probability p_6 for various nuclei that are considered in this work. These values are obtained by adding the probabilities in Ref. 17 for quark clusters larger than nucleons.

Nucleus	p_6
D	0.040
Be	0.095
O	0.146
Al	0.171
Fe	0.186
Pt	0.230
Au	0.230

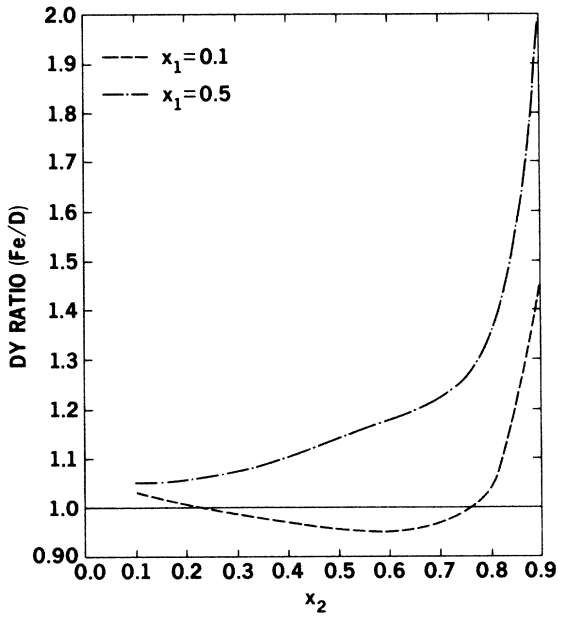

FIG. 1. QCM prediction for the ratio of proton-nucleus DY cross sections for Fe and D as a function of x_2. The two different choices of x_1 indicate where the ratio is sensitive to different ingredients of the QCM. For $x_1 = 0.1$ (0.5) the ratio is dominated by valence- (sea-) quark distributions of the target.

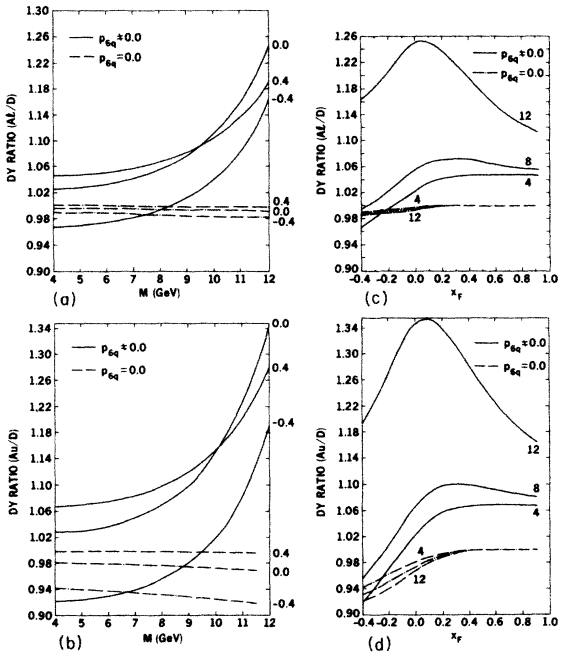

FIG. 2. Ratios of proton-nucleus DY cross sections at $\sqrt{s}=20.65$ GeV with and without six-quark clusters. (a) shows the ratio of Al to D as a function of M for three values of x_F. (b) is the same as (a) but for Au to D. (c) has the ratio for Al to D as a function of x_F for three values of M. (d) is the same as (c) but for Au to D.

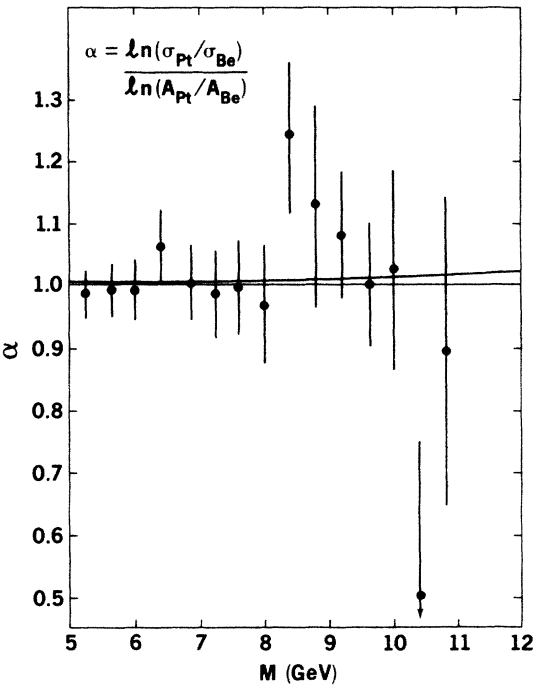

FIG. 3. Nuclear dependence of the DY cross section as a function of M. The data are taken from Ito *et al.* (Ref. 15). The solid line is the prediction of QCM.

the region of large M. We display typical enhancements for the values in the range $-0.4 \leq x_F \leq 0.4$. In Figs. 2(c) and 2(d) large enhancements are again observed for $M > 4$ GeV and $x_F > -0.2$. Note that for $x_F > 0.3$ the QCM predicts an M dependence to the DY ratio which disappears when p_6 is taken to be zero.

It is rather straightforward to understand the details of the enhancements in Fig. 2 based on the results of Fig. 1. $M=4$, 8, 12 (GeV) corresponds to $x_1=x_2=0.194$, 0.387, 0.581, respectively, when $x_F=0$ and $\sqrt{s}=20.65$ GeV. From Fig. 1, interpolating for x_1 and allowing for the appropriate change in p_6 (from Fe to Al), we obtain the enhancements shown in Fig. 2(a) for $x_F=0.0$. Similarly, the depletion at $x_F=-0.4$ and $M=4$ GeV shown in Fig. 2(c) corresponds to the depletion at $x_2 \simeq 0.5$ shown by the dashed curve in Fig. 1. We remind the reader that small-M results are more or less model independent, whereas large-M results depend strongly on the nature of the model. The large-M enhancement in our model is concentrated at x_F near zero which is the region easiest to probe experimentally. Even so, existing data with nuclear targets have error bars at large M which exceed the size of the effects shown here.

The ratio of the Fe and the nucleon antiquark distributions has been measured in a deep-inelastic neutrino scattering experiment.[13] The QCM results for this ratio are consistent with the data but the existing experimental error bars are so large as to admit practically any model.[1,5]

DY measurements of the sea quark (and hence the antiquark) distributions are as fundamental as the DIS measurements. Future DY experiments could provide determination of these ratios for $x < 0.4$ to a much higher accuracy than the existing neutrino measurements.[18] In the QCM these DY measurements could serve to fix what has, to this stage, been assumed for the gluon and sea-quark distributions.

B. A dependence

The A dependence of DY cross section is usually parametrized as A^α. For Pt and Be targets, cross sections can be cast in terms of α through

$$\alpha = \frac{\ln \sigma_{Pt}/\sigma_{Be}}{\ln A_{Pt}/A_{Be}} .$$

In Fig. 3 we compare the prediction of QCM with the data from Ito *et al.*[19] as a function of M for $x_F=0.0$. The experimentally extracted value of α is $1.007 \pm 0.018 \pm 0.028$. Once again large uncertainties in the data prevent us from drawing any definite conclusions.

C. Factorization

The major assumption behind the naive DY formula is the factorization hypothesis which ignores initial-state interactions. (For discussions see Refs. 20 and 21.) In a conventional multiple scattering approach, initial inelastic scattering of the projectile by the target particles prior to

the DY process will lead to a degradation of the beam momentum. We wish to explore the extent to which the possible presence of initial-state interactions would be offset by enhancements in cross sections due to $6q$ clusters. To get a qualitative estimate of the size of conventional hadronic multiple scattering effects we examine the A dependence of the DY ratio of Al to Be. In this estimate we take the average multiplicity as $\frac{3}{2}$ the observed multiplicity of charged particles in pp collisions at the same energy. Therefore, for $E_L=400$ GeV/c we find the center-of-momentum energy $\sqrt{s}$ is degraded by 5% for each of the first two inelastic collisions. We estimate that there are an average of 3 (2) inelastic collisions in an Al (Be) nucleus. Then using the average of cross sections we compute α. The results are given in Fig. 4 with and without $6q$ cluster contributions. The experimental observation that α is close to 1.0 in the relevant mass range is a clear indication of the absence of such initial state interactions *even when 6q cluster enhancements are included.* Combining the demonstrations in Figs. 3 and 4 we conclude that the present understanding of the lack of initial-state interactions based upon perturbative QCD (Refs. 20 and 21) is therefore consistent with the data even within the QCM.

D. Nuclear effects and the K factor

The experimental K factor is defined by

$$K=\frac{d\sigma/dM^2\,|_{\text{expt}}}{d\sigma/dM^2\,|_{\text{LLA}}},$$

where $d\sigma/dM^2\,|_{\text{LLA}}$ is the theoretical cross section calculated in the leading-logarithm approximation. For a QCD-based discussion of the K factor, see Refs. 22 and 23.

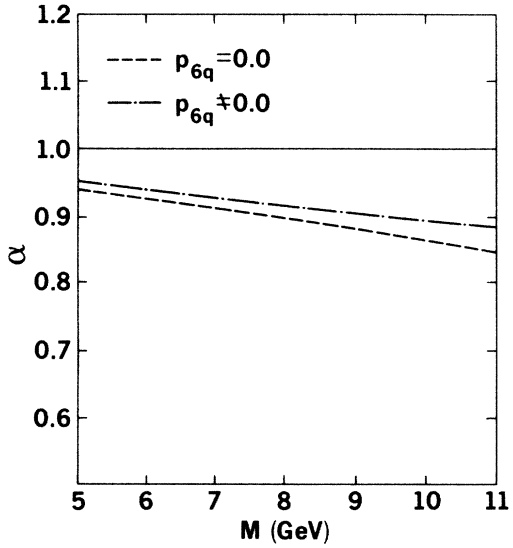

FIG. 4. Multiple-scattering effects (calculated in a conventional approach) for the nuclear dependence of the DY cross section.

Since the theoretical M^2 dependence of K is weak for the range of our calculations, we have treated K as an overall constant. The modifications of the quark distributions specified by the QCM would affect the K factor deduced from experiments with nuclear targets. To get an estimate of the uncertainties in the K factor due to nuclear effects within the QCM we have done the following analysis. A χ^2 analysis of the DY cross section is performed for the range of values $4.6\leq M\leq 8.0$ GeV and $0.025\leq x_F\leq 0.525$ for K ranging from 1.4 to 3.0 and for p_6 ranging from 0.0 to 0.4 using the recent NA3 data.[24] The result for χ^2/DF is presented in Fig. 5. If we accept a tolerance of a 3% change in χ^2 we have the freedom of the entire cross-hatched region in Fig. 5. Thus a value of $p_6=0.23$ together with $K=2.00$ does as well as $p_6=0$ and $K=2.13$. Therefore, the nuclear effects introduced via the QCM imply a 5—10% reduction in the K factor deduced from this data. This reduction however is small compared to the other theoretical and experimental uncertainties in the K factor. We present the comparison with experimental data for $M=5$ GeV in Fig. 6 where the two choices yield coincident curves. Greater sensitivity to p_6 in the proton-nucleus DY process has been shown above in Fig. 2 which covers a wider kinematic regime than the data summarized in the χ^2 analysis of Fig. 5.

E. The $x_2>1$ region

As mentioned earlier, it is possible to obtain DY cross-section ratios similar to DIS cross-section ratios by choosing x_1 to be small. Thus we saw in Fig. 1 a ratio similar to the EMC effect for $x_1=0.1$ in the region $x_2<1$. We now address the question of what happens when x_2 increases beyond 1. As shown in Fig. 7 the DY ratio in the QCM displays the same steplike character predicted for DIS (Ref. 25) and for the same reason. That is, in the region $1\leq x_2\leq 2$, the DY cross sections are dominated by the $6q$ cluster contributions so that the ratio of cross sections is approximately the ratio of $6q$ cluster probabilities, $p_6(\text{Fe})/p_6(\text{D})$. In this case, Table I indicates $p_6(\text{Fe})/p_6(\text{D})=4.7$ which explains the height of the plateau in Fig. 7.

Within the QCM the cross sections are nonzero out to x_2 approximately equal to the baryon number of the target. For successive integer increments of x_2 the cross-

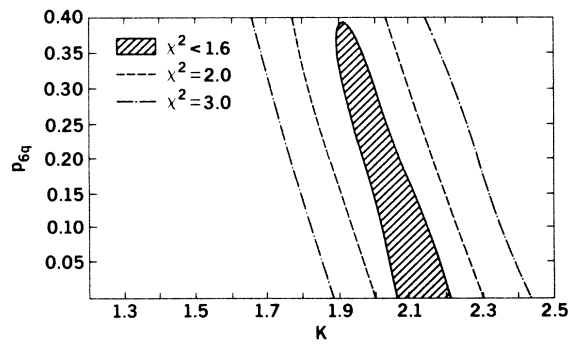

FIG. 5. χ^2/DF analysis of the the NA3 data (Ref. 20) for the $p+$Pt Dy process with p_6 and K as independent variables for $4.6\leq M\leq 8.0$ GeV and $0.025\leq x_F\leq 0.525$.

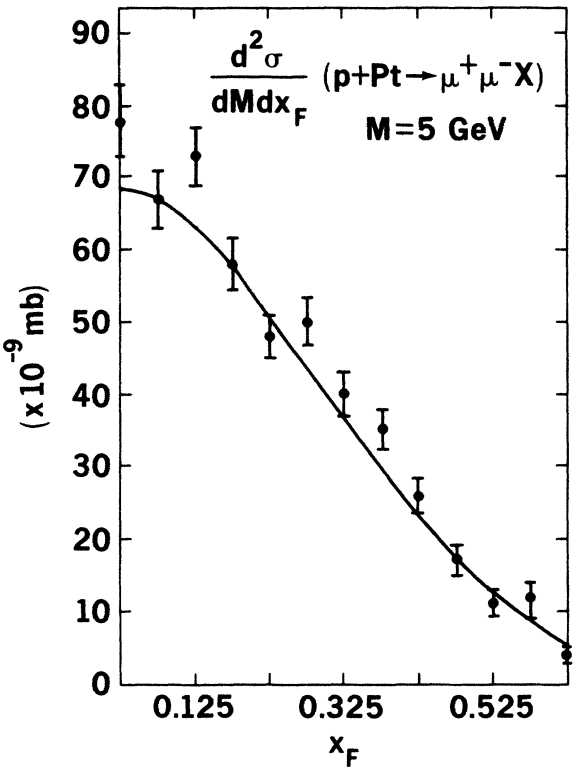

FIG. 6. Calculations for the choices (a) $K=2.13$, $p_6=0.0$ and (b) $K=2.0$, $p_6=0.23$ are compared with the NA3 data (Ref. 20) for the $p+$Pt DY process. The two calculated curves coincide in this figure.

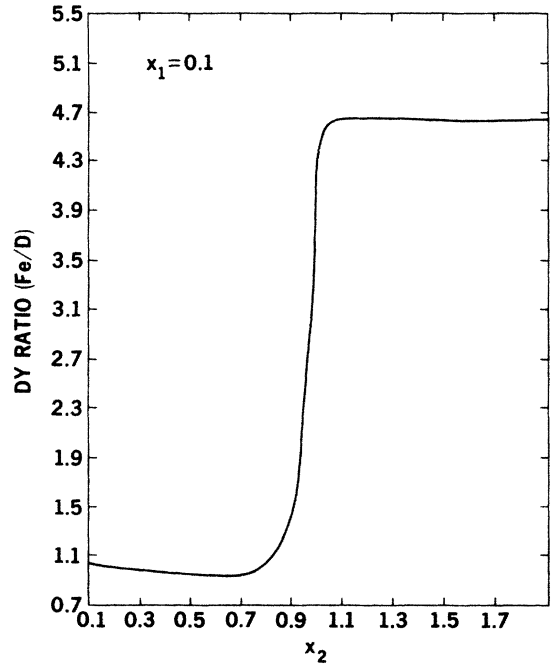

FIG. 7. QCM prediction for the ratio of DY cross sections for Fe and D as a function of x_2 (for $x_1=0.1$) in the region $0.1 \leq x_2 \leq 1.9$.

section ratios proceed to other plateaus whose magnitude is given by ratios of probabilities for successively larger clusters in these nuclei. In the present work we have approximated the QCM by absorbing higher cluster probabilities in p_6. A more complete treatment of the higher clusters yields $p_6(\text{Fe})/p_6(\text{D})=3.1$ using the results of Ref. 17.

IV. PION-NUCLEUS DRELL-YAN PROCESS

In this section we discuss the behavior of the ratio of cross sections for pion-nucleus DY process assuming a constant K factor. We restrict our considerations to $x_1>0.4$ and therefore neglect sea-quark distributions in the pion. Hence the pion-nucleus ratio of DY cross sections closely resembles the DIS cross-section ratio.[2,5] We have plotted the pion-nucleus DY cross-section ratio for Fe and D as a function of x_F for constant M in Fig. 8. Results are shown with and without six-quark clusters. Here, $s=(20.65\ \text{GeV})^2$. For this value of the c.m. energy and $M=4$ GeV, x_F varying from 0.0 to 0.8 corresponds to x_2 varying from 0.19 to 0.04. Thus as Berger[5] has pointed out, measurement of the ratio of cross sections in this kinematical domain is of great interest in the light of differences at low x among different DIS data[7,8] from nuclear targets.

V. NUCLEUS-NUCLEUS DRELL-YAN PROCESS

An interesting feature of the QCM is the indication of a partial deconfinement of quarks in nuclei. Thus quark cluster effects in hadronic dilepton production in heavy-ion collisions at relativistic energies may serve as a backdrop for signatures of the formation of exotic phases of matter like the quark-gluon plasma. Considerable interest

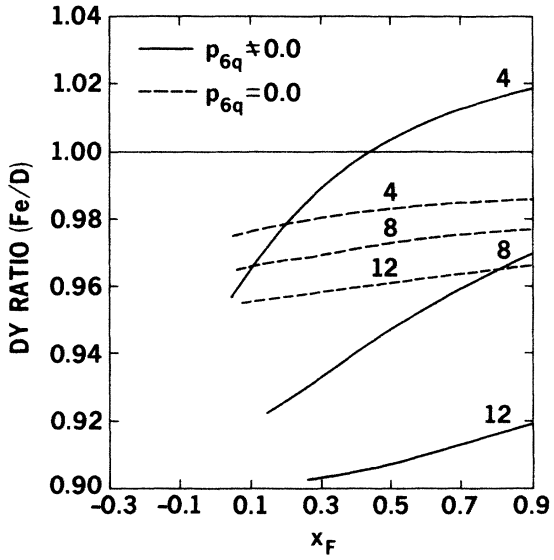

FIG. 8. Predictions for the ratio of pion-nucleus DY cross sections with and without six-quark clusters for Fe and D. The ratios are given as a function of x_F for three different values of M at $\sqrt{s}=20.65$ GeV.

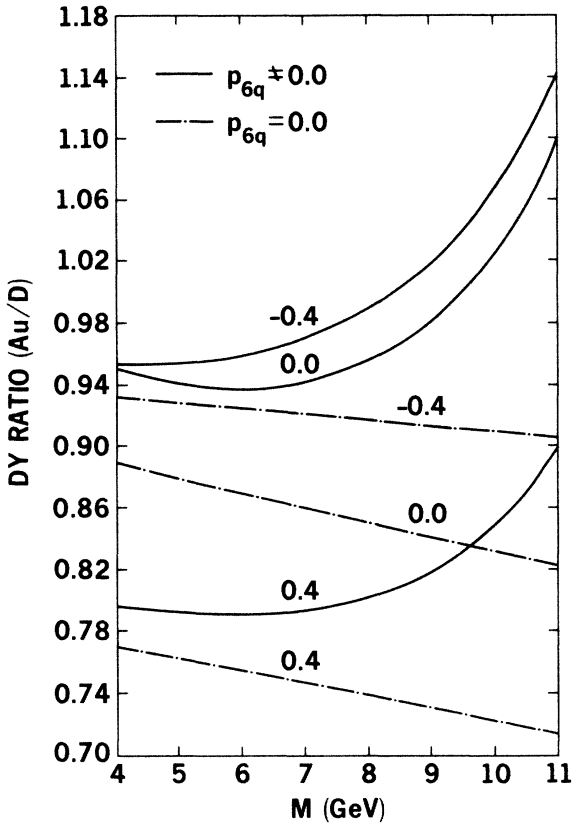

FIG. 9. Predictions for the ratio of O-Au to O-D cross sections with and without six-quark clusters for the DY process for a beam energy of 200 GeV per nucleon. The ratios are given as a function of M for three values of x_F.

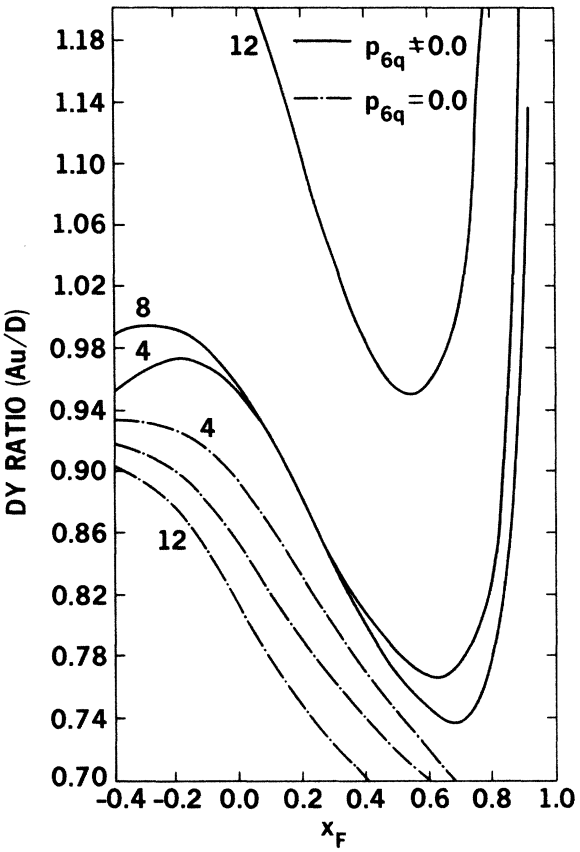

FIG. 10. Predictions for the ratio of O-Au to O-D cross sections with and without six-quark clusters for the DY process for a beam energy of 200 GeV per nucleon. The ratios are given as a function of x_F for three different values of M.

in these issues has been stimulated by the anticipation of oxygen beams up to 200 GeV per nucleon at CERN in the near future. We have seen that the QCM predicts enhancement of cross sections for the production of lepton pairs in the hadron-nucleus DY process. Because of the presence of six-quark clusters in both the projectile and the target, we expect very large enhancements in the cross section in certain kinematical regions. In Figs. 9 and 10 we present predictions for the ratio of O-Au to O-D cross sections for a beam energy of 200 GeV per nucleon. In Fig. 9 we display this DY ratio as a function of M for different values of x_F. For $M<7$ GeV a larger sensitivity to quark clusters is found for $x_F=0.0$. On the other hand, for $M>7$ GeV, sensitivity to quark clusters is observed for all values of x_F shown.

The ratio of DY cross sections for these same collisions is plotted as a function of x_F for fixed values of M in Fig. 10. Again, the stronger dependence on quark clusters is observed at larger M values. However, effects at the 10—20% level are found for $M=8$ GeV over the whole range $0.0\leq x_F\leq 0.6$. For a fixed projectile, changing the target does not change these enhancements dramatically. The reason is simply that we are performing an effective averaging over the same projectile.

CONCLUSIONS

We have evaluated the DY cross sections for lepton pair production in proton-nucleus, pion-nucleus, and nucleus-nucleus interactions within a simplified QCM. Some kinematical regions exhibit cross-section enhancement and others have cross-section suppression due to the role of six-quark clusters. We have examined the available data and have found that present uncertainties are too great to draw definite conclusions. That is, either the uncertainties in the present data or the lack of a theoretically precise determination of the K factor (or both) prohibit a direct test of the QCM. We have attempted to present results which indicate the kinematic regimes most sensitive to the ingredients of the QCM in the hope that this will stimulate further experimental work.

ACKNOWLEDGMENTS

We benefited greatly from discussions with Eli Rosenberg and Stan Brodsky. This work was supported in part by the U.S. Department of Energy under Contract No. DE-AC02-82ER40068, Division of High Energy and Nuclear Physics.

[1]R. P. Bickerstaff, M. C. Birse, and G. A. Miller, Phys. Rev. Lett. **53**, 2532 (1984); Phys. Rev. D **33**, 3228 (1986).
[2]T. Chmaj and K. J. Heller, Acta Phys. Pol. **B15**, 473 (1984); **B16**, 423 (1985).
[3]Y. Gabellini, J. L. Meunier, and G. Plaut, Z. Phys. C **28**, 123 (1985).
[4]N. P. Zotov, V. A. Saleev, and V. A. Tsarev, Pis'ma Zh. Eksp. Teor. Fiz. **40**, 200 (1984) [JETP Lett. **40**, 965 (1984)].
[5]E. L. Berger, Nucl. Phys. **B267**, 231 (1986).
[6]S. D. Drell and T.-M. Yan, Phys. Rev. Lett. **25**, 316 (1970); Ann. Phys. (N.Y.) **66**, 578 (1971). For extensive reviews that cover higher-order QCD effects see R. Stroynowski, Phys. Rep. **71**, 1 (1981) and I. R. Kenyon, Rep. Prog. Phys. **45**, 1261 (1982).
[7]J. J. Aubert *et al.*, Phys. Lett. **123B**, 275 (1983).
[8]A. Bodek *et al.*, Phys. Rev. Lett. **50**, 1431 (1983); **51**, 534 (1983); R. G. Arnold *et al.*, *ibid.* **52**, 727 (1984).
[9]G. Bari *et al.*, Phys. Lett. **163B**, 282 (1985).
[10]M. A. Parker *et al.*, Nucl. Phys. **B232**, 1 (1984).
[11]V. V. Ammosov *et al.*, Pis'ma Zh. Eksp. Teor. Fiz. **39**, 327 (1984) [JETP Lett. **39**, 393 (1984)].
[12]A. M. Cooper *et al.*, Phys. Lett. **141B**, 133 (1984).
[13]H. Abramovicz *et al.*, Z. Phys. C **25**, 29 (1984).
[14]H. J. Pirner and J. P. Vary, Phys. Rev. Lett. **46**, 1376 (1981); Nucl. Phys. **A358**, 413c (1981).
[15]C. E. Carlson and T. J. Havens, Phys. Rev. Lett. **51**, 261 (1983).
[16]H. J. Pirner, in *Particle and Nuclear Physics,* edited by A. Faessler (Pergamon, Oxford, 1985), p. 361; J. P. Vary, Nucl. Phys. **A418**, 195c (1984).
[17]M. Sato, S. A. Coon, H. J. Pirner, and J. P. Vary, Phys. Rev. C **33**, 1062 (1986).
[18]J. Moss, in LAMPF Workshop on Quark/Gluon Phenomena in Nuclear and Particle Physics, Los Alamos, New Mexico, 1986 (unpublished).
[19]A. S. Ito *et al.*, Phys. Rev. D **23**, 604 (1981).
[20]A. H. Mueller, in *Proceedings of the Drell-Yan Workshop, Fermilab, 1982,* edited by E. L. Berger, P. Malhotra, R. Ovara, and H. Thacker (Fermilab, Batavia, IL, 1982).
[21]S. J. Brodsky, in *Progress in Physics* edited by A. Jaffe, G. Parisi, and D. Ruelle (Birkhauser, Boston, 1983), Vol. 8, p. 1.
[22]G. Altarelli, R. K. Ellis, and G. Martinelli, Nucl. Phys. **B157**, 461 (1979).
[23]W. J. Stirling in *Proceedings of the Drell-Yan Workshop, Fermilab, 1982* (Ref. 20).
[24]J. Badier *et al.*, Z. Phys. C **26**, 489 (1984).
[25]J. P. Vary, in *Proceedings of the VII International Seminar on Higher Energy Physics Problems, Multi Quark Interactions, and Quantum Chromodynamics,* edited by V. V. Burov (Dubna Pub. No. D-1, 2-84-599, 1984), p. 186.